Mechanism and substrate specificity of the flavin reductase ActVB from Streptomyces coelicolor.

Laurent Filisetti, Marc Fontecave, Vincent Niviere

Mechanism and Substrate Specificity of the Flavin Reductase ActVB from *Streptomyces coelicolor*

Laurent Filisetti, Marc Fontecave*, and Vincent Nivière *

Laboratoire de Chimie et Biochimie des Centres Redox Biologiques, DRDC-CEA/CNRS/Université Joseph Fourier, 17 Avenue des Martyrs, 38054 Grenoble, Cedex 9, France.

* To whom correspondence should be addressed. Vincent Nivière; Tel. : 33-4-38-78-91-09; Fax : 33-4-38-78-91-24; E-mail : vniviere@cea.fr. Marc Fontecave; Tel. : 33-4-38-78-91-03; Fax : 33-4-38-78-91-24; E-mail : mfontecave@cea.fr.

Running title : Substrate Specificity of the Flavin Reductase ActVB

SUMMARY

ActVB is the NADH:flavin oxidoreductase participating in the last step of actinorhodin synthesis in *Streptomyces coelicolor*. It is the prototype of a whole class of flavin reductases with both sequence and functional similarities. The mechanism of reduction of free flavins by ActVB has been studied. Although ActVB was isolated with FMN bound, we have demonstrated that it is not a flavoprotein. Instead ActVB contains only one flavin binding site, suitable for the flavin reductase activity and with a high affinity for FMN. In addition, ActVB proceeds by an ordered sequential mechanism, where NADH is the first substrate. Whereas ActVB is highly specific for NADH, it is able to catalyze the reduction of a great variety of natural and synthetic flavins, but with K_m values ranging from 1 (FMN) to 69 (lumiflavin) μM. We show that both the ribitol-phosphate chain and the isoalloxazine ring contribute to the protein-flavin interaction. Such properties are unique and set the ActVB family apart from the well-characterized Fre flavin reductase family.

INTRODUCTION

NAD(P)H :flavin oxidoreductases or flavin reductases are enzymes defined by their ability to catalyze the reduction of free flavins, riboflavin, flavin mononucleotide (FMN) or flavin adenine dinucleotide (FAD), by reduced pyridine nucleotides, NADPH or NADH (1). As flavins do not bind tightly to them, flavin reductases should not be classified as flavoproteins. What the enzyme does is to provide an active site that transiently accommodates both the reduced pyridine nucleotide and the flavin, close to each other, in such a relative orientation, that the direct hydride transfer can be enormously accelerated (2, 3). The real biological function of the reduced flavins, the released products of the catalyzed reaction, is still not well understood. Free reduced flavins have been suggested to play an important role as redox mediators in iron uptake and metabolism in prokaryotes (4) or in light emission in bioluminescent bacteria (5, 6). More recently a group of flavin reductases has been found to be essential in combination with flavin-dependent oxygenases (7-13), such as those involved in antibiotic biosynthesis, as discussed below (7-9).

Organisms have evolved a great variety of such enzymes, which can thus be classified within several families or subfamilies according to their sequence similarities and biochemical properties. Because of their simplicity and their variety, flavin reductases thus provide a unique tool to understand how a polypeptide chain deals with both the isoalloxazine ring and the ribityl chain of

a flavin molecule to modulate its binding constant, to accelerate its reduction by reduced pyridine nucleotide and to use it for a diversity of functions. Surprisingly, our knowledge of this class of enzymes is very limited so far and this is the reason why flavin reductases have been the subject of intensive investigations in our laboratory in the recent years (3, 14-17).

The prototype of one group of flavin reductases is the Fre enzyme found in *Escherichia coli* (18) and also in luminescent bacteria (19). The enzyme from *E. coli* consists of a single polypeptide chain with a molecular mass of 26 kDa. It uses both NADPH and NADH as the electron donor and a great variety of flavin analogues as electron acceptors (14, 17). This clearly demonstrates that the recognition of the flavin by the polypeptide chain occurs exclusively through the isoalloxazine ring, with very limited contribution of the ribityl side chain (3, 14). The crystal structure of Fre (3) reveals that the general enzyme structure is, despite very low sequence similarities, similar to the structures of a large family of flavoenzymes, with spinach ferredoxin-$NADP^+$ reductase (FNR) as the prototype (20). It provides insights to the understanding of the structural basis for the difference in flavin recognition between a flavoprotein and a flavin reductase.

A second group of flavin reductases, different from the Fre family and the flavin reductases purified from bioluminescent bacteria, has recently emerged (7-13). However, very few members of this group were purified to homogeneity and carefully characterized. These enzymes are defined on the

basis of their amino acid sequence similarities and their role during biological oxidation reactions. Indeed some monooxygenase systems depend on the presence of a reduced flavin, mainly $FMNH_2$, as a co-substrate rather than a prosthetic group. The flavin is supposed to react with molecular oxygen in the active site of the monooxygenase component in order to generate a flavin hydroperoxide intermediate that serves as the active oxidant for substrate oxidation. A separate flavin reductase is thus absolutely required to supply the reduced flavins (with NADPH or NADH as the reductant) that diffuse to the oxygenase component. In the recent years the following flavin reductases have been shown to belong to this family: ActVB (7), SnaC (8) and VlmR (9) for the biosynthesis of the antibiotics actinorhodin in *Streptomyces coelicolor*, pristinamycin in *Streptomyces pristinaespiralis* and valanimycin in *Streptomyces viridifaciens*; HpaC (10) for the oxidation of 4-hydroxyphenylacetate in *E. coli* ; DszD (11) for the conversion of sulfides to sulfoxides and sulfones in *Rhodococcus sp.* allowing the utilization of these microorganisms in fossil fuel desulfurization biotechnological processes; cB (12) for the degradation of nitrilotriacetate in *Chelatobacter heintzii* . It should be noted that a flavin reductase called Fer (21, 22), with some homology to ActVB and SnaC, found as a ferric reductase in the hyperthermophilic archaea *Archaeoglobus fulgidus*, has been structurally characterized in complex with FMN (22).

Considering the biological importance of this group of flavin reductases and the very limited amount of available information regarding their substrate specificity, reaction mechanisms and three-dimensional structure, we found worth characterizing these enzymes in more detail in order to compare them to the Fre enzyme and get new insights to the general understanding of the protein-flavin interaction. We have chosen ActVB as a representative of this group of flavin reductase and report original data showing that ActVB has a unique mode of flavin binding and operates by a sequential mechanism.

EXPERIMENTAL PROCEDURES

Enzyme Assay. In the standard aerobic assay, flavin reductases activities were carried out under aerobic conditions allowing continuous reoxidation of reduced flavin by oxygen. Flavin reductase activity was determined at 25 °C from the decrease of the absorbance at 340 nm (ε_{340nm}= 6.22 mM^{-1} cm^{-1}) due to the oxidation of NADH, using a Varian Cary 1 Bio spectrophotometer. Under standard conditions, the spectroscopic cuvette contained, in a final volume of 500 µl, 50 mM Tris/HCl, pH 7.6, 100 µM NADH and 50 µM FMN. The reaction was initiated by adding 0.5-1 µg of enzyme. Enzyme activities were determined from the linear part of the progress curve, with less than 10% of reduced pyridine nucleotide utilized over the time course of the reaction. One

unit of activity is defined as the amount of protein catalyzing the oxidation of 1 μmol of NADH per min. When high concentrations of NAD(P)H were investigated, a 0.1 cm path length cuvette was used (final volume 0.3 ml). The hydrophobic flavin analogues lumichrome, alloxazine and lumiflavin were dissolved in 100 % Me_2SO and the enzymatic assays thus contained 90 mM Me_2SO, final concentration. Me_2SO concentrations up to 500 mM had no measurable effect on K_m and V_m values.

NAD(P) analogs and flavin concentrations were determined spectroscopically using the following extinction coefficients : AMP and ADP-ribose, ε_{259nm}= 15.4 mM^{-1} cm^{-1}; ß-$NAD(P)^+$, ε_{259nm}= 17.8 mM^{-1} cm^{-1}; NMNH, ε_{338nm}= 5.72 mM^{-1} cm^{-1}; riboflavin and FMN, ε_{450nm}= 12.5 mM^{-1} cm^{-1}; FAD, ε_{450nm}= 11.3 mM^{-1} cm^{-1}; lumichrome, ε_{356nm} = 6.0 mM^{-1} cm^{-1}.

ActVB expression plasmids. For the production of wild-type ActVB, pACTVB plasmid was used (7), where *actVB* structural gene was placed under the control of the T7 polymerase promotor, in the pT7-7 plasmid. For the production of ActVB-His as C-terminal histidine-tagged fusion protein, the *actVB* gene was amplified by PCR from the plasmid pACTVB (7) with the oligonucleotide primers GGGAATTCCATATGGCTGCTGACCAGG and CGCGGATCCTCA*ATGGTGATGGTGATGGTG*ACCGGCATGCGCGGGCA C, in order to introduce *EcoR*I, *Nde*I and *BamH*I restriction sites (underlined) and the 6 histidine codons (italics). The 549-base pairs PCR product was

digested with *EcoR*I-*BamH*I and the resulting fragment was ligated in pUC18 (pUC18-ActVB). This plasmid was sequenced to confirm that no changes had been introduced during PCR amplification. The *Nde*I-*BamH*I fragment from pUC18-ActVB was subsequently cloned in pT7-7 resulting in the plasmid pACTVB his-tag.

Preparation of soluble extracts. *E. coli* B834(DE3) pLysS transformed with the appropriate plasmid (pACTVB or pACTVB his-tag) was grown at 37°C and 220 rpm in a 3-liter Erlenmeyer flask containing 1 liter of Luria-Bertani medium in the presence of 200 μg/ml ampicillin and 34 μg/ml chloramphenicol. Growth was monitored by following the absorbance at 600 nm. Expression of ActVB and ActVB-His recombinant proteins was induced by adding IPTG to a final concentration of 250 μM when the optical density of the culture was about 0.3. To minimize the formation of insoluble protein aggregates, cultures were cooled to 25°C after addition of IPTG and then further grown for 5 h. Cells were collected by centrifugation for 10 min at 6500xg at 4°C. Extraction of soluble proteins was performed by lysozyme digestion and freeze-thawing cycles, in the presence of antiprotease complete™ buffer. All of the following operations were performed at 4°C. After ultracentrifugation at 45,000 rpm during 90 min in a Beckman 60 Ti rotor, the supernatant was used as soluble extracts for purification.

Purification of ActVB. The soluble extracts (130 mg) were loaded onto an ACA54 column (360 ml) previously equilibrated with 10 mM Tris/HCl, pH 7.6,

10% glycerol, 10 mM EDTA. Proteins were eluted with a flow rate of 0.3 ml/min. Fractions containing flavin reductase activity were pooled and concentrated to 2 ml using a Diaflo cell equipped with a YM 10 membrane. The concentrated enzyme solution was loaded onto a Superdex 75 column (120 ml from Pharmacia) equilibrated with 25 mM Tris/HCl pH 7.6, 10% glycerol, 10 mM EDTA (buffer A). Proteins were eluted with the same buffer at a flow rate of 0.8 ml/min. Fractions containing flavin reductase activity were pooled and loaded onto a UNO Q column (6 ml, Bio-Rad), equilibrated with buffer A. A linear 0-500 mM NaCl gradient in buffer A was applied for 60 ml. ActVB was eluted with 100 mM NaCl.

Purification of ActVB-His. The soluble extracts (180 mg) were loaded at 0.5 ml/min onto a 25 ml Ni-NTA column (Qiagen) equilibrated with 50 mM Tris/HCl pH 7.6 (buffer B). Then, the column was washed with 100 ml of buffer B and elution was achieved with 100 mM imidazole in the same buffer at 1 ml/min. The proteins were then immediately loaded onto a UNO Q column (6 ml, Bio-Rad), and further eluted with a linear 0-500 mM NaCl gradient in buffer B for 60 ml, at 1 ml/min.

Analytical determination. SDS-PAGE polyacrylamide gels (15% polyacrylamide) were done according to Laemmli (23). The gels were calibrated with the Pharmacia low molecular weight markers. The native molecular mass of the protein was determined with a Superdex 75 gel filtration column (120 ml, Pharmacia) equilibrated with 25 mM Tris/HCl, pH

7.6 and 150 mM NaCl using a flow rate of 0.4 ml.min^{-1}. Bovine serum albumin (66 kDa), ovalbumin (45 kDa), trypsine inhibitor (20.1 kDa) and cytochrome c (12.4 kDa) were used as the markers for molecular mass. The void volume was determined with ferritin (450 kDa). Protein concentration was determined using the Bio-Rad protein assay reagent (24) with bovine serum albumin as a standard. Anaerobic experiments were carried out in a Jacomex glove box equipped with an HP 8453 diode array spectrophotometer coupled to the measurement cell by optical fibers (Photonetics system).

Cofactor analysis. A sample of pure ActVB or ActVB-His protein was boiled for 10 min in the dark, chilled on ice and then centrifuged for 10 min at 10,000xg in order to pellet the denatured protein. An aliquot of the supernatant was analyzed both by UV-visible spectroscopy and by thin-layer chromatography on silica gel 60 F254 (Merck) with butanol-1/acetic acid/water (10/5/5) as the eluant. As a control, pure FMN, FAD and riboflavin were run separately or as a mixture, under the same conditions.

Kinetic analysis. The molar concentration of ActVB was calculated assuming a molecular weight value of the polypeptide chain of 18,260 Da (7). Reciprocal initial velocities ($1/v_i$) were plotted against reciprocal substrate concentrations (1/[S]) and fitted with a straight line determined by a linear regression program. In some cases, kinetic parameters (V_m, K_m, K_{mapp}) were determined from saturation curves, fitted with the equation: $v_i=(V_m[S])/(K_m+[S])$, using a Levenberg-Marquardt algorithm. Inhibition constants (K_i) for competitive

inhibitors were determined using a secondary plot of the slopes from the double reciprocal plots against the concentration of the inhibitor [I], corresponding to the equation: $y = (K_m/V_m)(1+([I]/K_i))$ (25). In the cases of noncompetitive and uncompetitive inhibitors, the inhibition constant (K_i) was determined using a secondary plot of the intercepts from the double reciprocal plot against the concentration of the inhibitor [I], corresponding to the equation: $y = (([I]/(K_i V_m)) + 1/V_m$ (25). When applicable, values are shown ± standard deviation.

RESULTS

Purification of ActVB

In a first set of experiments, ActVB was overexpressed in *E.coli* using the pACTVB plasmid (7). Using the purification procedure described in the experimental section, a low yield (6-7 %) of purified ActVB could be obtained (Table I, A). This was then explained by the great instability of the flavin reductase activity in the soluble extracts. The activity, routinely assayed from the oxidation of NADH by an excess of FMN monitored spectrophotometrically, was found to decrease by 50 % when the protein was left in buffer for 3 hours at 4 °C. Addition of 10% glycerol, 10 mM EDTA and ™complete buffer solution to the soluble extracts provided a significant stabilization of the activity (data not shown). However, even under these

conditions, more than 90 % of the flavin reductase activity was lost during the first two chromatographic steps (Table I, A). After the UNO Q column, activity remained stable, suggesting that instability of ActVB activity in soluble extracts arose from reactions with some cellular components. SDS-PAGE analysis after the UNO Q purification step revealed the presence of two polypeptide bands at 18,000 and 17,000 Da (data not shown), with the same AADQGMLRDA N-terminal sequence corresponding to the ActVB protein (7). This suggested a partial C-terminal proteolysis of ActVB when expressed in *E. coli*, as described previously (7). In contrast, overexpression of ActVB as a C-terminal his-tagged fusion protein (ActVB-His) allowed a more efficient purification of the enzyme (Table I, B). SDS-PAGE analysis after the UNO Q column revealed the presence of only one polypeptide chain at 18,000, without evidence for partial proteolysis (data not shown).

Gel-filtration experiments on Superdex 75 column with ActVB and ActVB-His gave an apparent molecular mass of 36,000 Da for both proteins, confirming the homodimeric structure for ActVB (7).

Flavin reductase specific activities of both ActVB and ActVB-His proteins were found to be comparable (Table I), indicating that the C-terminal part of the protein lost during proteolysis was not important for activity and that the presence of the His-tag was neutral with regard to the enzyme activity. However, it should be noted that from one preparation to another, we obtained purified proteins with slightly different specific flavin reductase activities.

In the following experiments presented here, we report data obtained with ActVB. In the case of the kinetic experiments, the same enzyme preparation was used allowing a direct comparison of the parameters obtained under different kinetic conditions.

Flavin content of ActVB

Purified ActVB was yellow, with absorption spectra typical for a flavin-containing protein, with maxima at 378 and 455 nm (Fig. 1). After denaturation of the protein by boiling for 10 min and centrifugation, the chromophore contained in the supernatant was analyzed by thin-layer chromatography, with FMN, riboflavin and FAD as standards. The chromophore was identified as FMN (data not shown). Quantification of the free FMN released in the supernatant by UV-visible spectroscopy demonstrated that the amount of FMN in purified ActVB varied from one preparation to another from 0.1 to 0.6 mol of FMN per mol of polypeptide chain. An extinction coefficient of 13,640 $M^{-1}cm^{-1}$ at 455 nm for the bound FMN was calculated.

Reconstitution experiments of ActVB with FMN or riboflavin gave the following results. A preparation of ActVB (50 μM) containing little FMN (0.1 mol FMN per mol of protein) was incubated with 1 mM FMN or 400 μM riboflavin for 1 hour in 50 mM Tris/HCl buffer pH 7.6 and then chromatographied on a NAP10™ column (Pharmacia) in order to remove unbound flavin. The protein was then analyzed both by UV-visible

spectroscopy and thin-layer chromatography, as previously described, in order to identify and quantify the bound flavin in the reconstituted ActVB. Reconstitution with FMN resulted in a 6-7-fold increase of the amount of protein-bound FMN and a protein containing 0.6 to 0.7 mol FMN per mol of protein (data not shown). In contrast, reconstitution with riboflavin failed to increase the amount of protein bound flavin and did not result in the removal of FMN initially bound to ActVB (data not shown).

Titration of the ActVB FMN bound by NADH

In order to verify that the FMN bound to the isolated ActVB protein was correctly located at the flavin reductase active site, reductive titration of FMN was carried out with NADH, under anaerobic conditions. A preparation of ActVB containing 0.5 mol of FMN per mol of ActVB polypeptide chain (18,260 Da) was used for that experiment. As shown in Fig. 2, addition of NADH caused a decrease in the absorbance at 455 nm, reflecting a reduction of FMN. An isosbestic point at 510 nm was observed for substoichiometric concentrations of NADH. In the inset of Fig. 2, a plot of the fractional absorbance changes at 445 nm as a function of [NADH]/[FMN] ratio showed that 1 mole of NADH was sufficient to reduce 1 mol of bound FMN. In addition, during the NADH titration, a broad absorption band above 550 nm developed (Fig. 2). Such a band is tentatively assigned to a charge-transfer complex of reduced FMN with NAD^+ within the active site of ActVB rather

than to a flavin neutral semiquinone species (26, 27), as confirmed by the following experiment (Fig. 3). An anaerobic solution of ActVB, containing 0.5 mol of bound FMN per mol of polypeptide chain, EDTA and catalytic amount of deazaflavin was photoreduced and then titrated with increasing amounts of NAD^+. As shown in Fig. 3, irradiation resulted in the decrease of the absorbance at 455 nm, consistent with reduction of FMN by photoreduced deazaflavin. When NAD^+ was added, a broad band developed at wavelengths greater than 520 nm, which was similar to that observed during reaction of ActVB-bound FMN with NADH. In addition, no significant increase in absorbance at 340 nm was observed, indicating that no NADH was formed during incubation of reduced FMN with NAD^+. This shows that the reduction of FMN by NADH at the active site of ActVB is irreversible.

Flavin reductase activity is not dependent on the bound FMN

The previous experiments have shown that the purified protein contains various amounts of FMN bound at its active site, depending on the enzyme preparation. In order to investigate the dependence of the flavin reductase activity of ActVB on the amount of protein-bound FMN, different preparations containing various amounts of FMN were assayed either with FMN or riboflavin as a substrate and with NADH as the electron donor (Table II). In the absence of exogenous flavins, only a very weak activity could be detected (data not shown), excluding a NADH oxidase function for ActVB. With either FMN

or riboflavin as a substrate, the flavin reductase activity of ActVB was found to be independent on the FMN content of the polypeptide chain (Table II). Since riboflavin does not bind to ActVB (see above), reconstitution for a flavin site during the enzymatic test is excluded. These observations thus rule out the possibility that the protein-bound FMN was involved in the flavin reductase activity and are consistent with ActVB being a flavin reductase accepting both FMN and riboflavin as substrates. It is likely that, under the assay conditions, the protein-bound FMN can be displaced by the large excess of riboflavin.

Kinetic analysis of ActVB

The dependence of the reaction catalyzed by ActVB on the concentration of both substrates, flavin and reduced pyridine nucleotide, was investigated by kinetic experiments under steady-state conditions. For all the following kinetic experiments, the same homogeneous enzyme preparation was used. For such a bisubstrate-biproduct reaction, kinetic analysis provides insights into the mechanism. Double reciprocal plots of initial velocities versus substrate concentrations show intersecting patterns in the case of a sequential mechanism and parallel patterns for a ping-pong mechanism (25). Flavin reductase activity was determined as a function of NADH concentration at several levels of FMN (Fig. 4A) and as a function of FMN concentration at several levels of NADH (Fig. 4B). Initial velocities followed typical Michaelis-Menten kinetics since double reciprocal plots of the data showed a series of lines. Moreover, a ping-

pong mechanism could be excluded since the lines were intersecting each other at the same point at the left of the vertical axis. A sequential mechanism for ActVB is thus indicated (25). However whether it is an ordered or a random sequential mechanism cannot be concluded from such an experiment. It may be experimentally deduced from the inhibition studies described below (28).

When the enzyme activity was determined as a function of NADH concentration in the absence or in the presence of three concentrations of adenosine 5'-monophosphate (AMP, Scheme 1), a dead-end inhibitor, double reciprocal plots revealed typical competitive inhibition kinetics (Fig. 5A). A K_i value of 3 ±0.5 mM was obtained for AMP. On the other hand, a pattern of non-competitive inhibition was observed for AMP with respect to the FMN substrate, with a K_i value of 7.7 ±0.4 mM [1] (Fig. 5B). Furthermore, lumichrome, a flavin analogue (Scheme 1) with no redox activity, was a competitive inhibitor with respect to FMN with a K_i value of 104 ±17 μM (Fig. 6A) and an uncompetitive inhibitor with respect to NADH, with a K_i value of 91 ±1 μM (Fig. 6B). All these data support the conclusion that the flavin reductase has an ordered mechanism with NADH binding first and FMN being the second substrate (28).

The kinetic mechanism of product release has been determined by studying inhibition by products (25). When NADH concentration was varied

[1] For a two-substrate enzyme, the K_i values for an inhibitor with respect to each substrate should not be necessary equal (25).

with a fixed concentration of FMN, inhibition by NAD^+ was found to be non-competitive with respect to NADH (data not shown). When FMN was varied at a fixed NADH concentration, NAD^+ appeared to inhibit non competitively (data not shown). This now suggests that the first product to be released is NAD^+, followed by the reduced flavin.

Flavin substrate specificity

Scheme 1 shows the structures of the various flavin analogs used as substrates or inhibitors. Table III reports the kinetic parameters for each substrate obtained during enzymatic reduction by NADH under steady-state conditions. The apparent K_m values were determined in experiments where flavin reductase activities were measured as a function of the concentration of a given substrate in the presence of saturating concentrations of the other substrate. In addition, the K_m and k_{cat} values for the FMN substrate were determined from the data shown in Figures 4A and 4B, using the Dalziel treatment which is well adapted for a sequential bireactant mechanism (29, 16-17). The latter were found to be 0.78 ±0.10 μM and 8.9 ±0.3 s^{-1} respectively, which are comparable to those reported in Table III.

As shown in Table III, V_{max} values (reported as k_{cat} values) were only slightly sensitive to modifications of the flavin moiety both at the isoalloxazine ring and the ribityl side chain. On the contrary, K_m values for the flavin substrate strongly depended on the nature of the substituent at the N-10 position

of the isoalloxazine ring. As previously reported in (7), FMN was found to be the best substrate, with a K_m value of 1 μM. Riboflavin and FAD exhibited a 8-fold larger K_m value, suggesting that the terminal phosphate group on the ribityl chain of the FMN molecule provided significant stabilization of the flavin-protein complex. Lumiflavin, with a methyl group at N-10 position, was also a substrate of ActVB, although its K_m value was much larger than that for FMN, FAD or riboflavin. This shows the importance of the isoalloxazine ring for the flavin-protein recognition, in agreement with lumichrome and alloxazine being competitive inhibitors of FMN, with K_i values of 104 and 93 μM, respectively (Fig. 6A and Table III).

In the case of a sequential ordered mechanism, the K_d value for a competitive inhibitor with respect to the second substrate can be calculated from its K_i value according to the following equation : $K_d = K_i /(1 + K_{d\ NADH}/[NADH])$ (30), where $K_{d\ NADH}$ is the dissociation constant for the first substrate NADH and [NADH] the concentration of NADH used to determine the K_i value. Using $K_{d\ NADH}$ = 7.8 ±0.7 μM (see below), K_d values for lumichrome and alloxazine of 87 ±14 and 78 ±18 μM, respectively, could be obtained. The K_d value for lumichrome value is comparable to the K_m value for lumiflavin (69 ±8 μM), its closest flavin substrate analogue. This suggests that K_m values for the flavin substrates represent good approximations for the corresponding K_d values during catalysis.

The role of the ribityl chain in the flavin-protein interaction was further investigated with flavin analogs carrying different substituents at the N-10 position (Scheme 1 and Table III). Since binding of the flavin molecule seems to involve the ribityl-phosphate chain as well, we have examined the role of the OH ribityl groups in that recognition (Table III). K_m values for flavins were in that other: 1 < riboflavin < 3 < 2 < lumiflavin. Furthermore, in the case of compound 2, the k_{cat} value was significantly decreased with regard to k_{cat} values with 3 and riboflavin. Those data suggest that the 2'-OH contributes to the protein-flavin recognition, whereas the 3'-OH plays a minor role. It should be noted that ribitol, up to 10 mM, is not an inhibitor (data not shown).

Reduced pyridine nucleotide substrate specificity

Table IV shows the kinetic and thermodynamic parameters for various NAD(P)H analogs (Scheme 1) obtained during enzyme reaction under steady-state conditions. The K_m value for the NADH substrate was also determined from the data shown in Figures 4A and 4B, using the Dalziel treatment (29, 16-17), and found to be 9.7±0.4 μM, which is comparable to the value reported in Table IV. As previously reported in (7), ActVB is strictly specific for NADH. NADPH cannot be used as a substrate, even at very high concentrations (up to 0.8 mM). The K_m value for NADH (6.6 ± 0.5 μM, Table IV) was comparable to its K_d value (7.8 ± 0.7 μM) determined from the Dalziel mathematical treatment of the initial velocities data reported in Fig. 4A and 4B (29, 16-17). K_i values

for AMP and ADP-ribose, which are competitive inhibitors with respect to NADH (Fig 5A and not shown, respectively), were very large (3 and 17.4 mM, respectively, Table IV). In the case of a sequential ordered mechanism, the inhibition constant K_i for a competitive inhibitor with respect to the first substrate is equal to the dissociation constant of the enzyme-inhibitor complex (30). Comparison of the K_i values for AMP and ADP-ribose with the K_d value for NADH thus indicates that the nicotinamide ring plays a major role in the binding of NADH molecule to ActVB. On the other hand, NMNH, the NADH analog lacking the AMP part of the molecule (Scheme 1), was neither a substrate nor an inhibitor, up to a concentration of 1 mM (Table IV). This now indicates that the nicotinamide ribose phosphate part of the NADH is not recognized by itself either. Taken together, these data suggest that the NADH molecule is recognized by ActVB as a whole and that individual contributions of the different parts of the molecule cannot provide enough interactions unless they are associated with the other parts of the NADH molecule.

DISCUSSION

The enzyme named Fre can be considered as a prototype of a whole class of flavin reductases, the enzymes catalyzing the reduction of riboflavin, FMN and FAD by NADPH and NADH (14). This is the most extensively characterized flavin reductase so far (2, 3, 14, 16-18). Kinetic analysis and structural characterization in our laboratory have shown that this enzyme binds the flavin, with a preference for riboflavin, almost exclusively through interactions with the isoalloxazine ring (14) and reduced pyridine nucleotides, preferably NADPH, mainly through interactions with the nicotinamide moiety (17). These are unique binding modes. The enzyme proceeds by a sequential ordered mechanism, binding the NADPH first and providing a site that accommodates both substrates in a ternary complex from which the optimized hydride transfer occurs (2, 14).

ActVB belongs to a different and much less well-characterized group of flavin reductases. These enzymes are generally associated to flavin-dependent monooxygenases and have no sequence homology with the Fre family (7-13). Here we report a detailed study of ActVB that allows comparison to Fre. As discussed below we show that ActVB is different from Fre also with respect to substrate specificities and recognition.

The first question we have addressed is whether ActVB is a flavoprotein or not. Previous reports had not provided a clear answer to that question and

furthermore in our hands preparations of ActVB had highly variable amounts of protein-bound FMN. Furthermore, whereas some members of the ActVB family, such as HpaC (10), were isolated without bound cofactors others, such as SnaC (8), were shown to contain significant amounts of flavin bound to the polypeptide chain after purification. The presence of FMN in ActVB could be explained either by a tight interaction between ActVB and FMN allowing isolation of the flavin reductase with its substrate or by a loss of a prosthetic FMN group from a flavoprotein during purification. It should be noted that some flavoproteins, such as sulfite reductase, may display some flavin reductase activity (15). However in this case, the internal flavin cofactor mediates an unspecific electron transfer from NAD(P)H to the exogenous flavin substrate as well as other acceptors (quinones, ferric iron, cytochrome c…) and thus proceeds through a ping-pong mechanism (15).

The results presented here unambiguously demonstrate that ActVB is not a flavoprotein but a flavin reductase displaying a low K_d value for FMN. First, with all substrates, FMN, riboflavin and FAD, the kinetic data nicely fit with a sequential and not with a ping-pong mechanism (Fig. 4). Second, FMN and riboflavin reductase activities do not depend on the amount of FMN bound to the protein used for the assay (Table II). Third, ActVB cannot bind more than one equivalent of FMN as shown by reconstitution experiments, in agreement with the presence of only one FMN binding site. Furthermore, this site is

directly accessible to NADH where electron transfer can occur as shown from the formation of a charge transfer complex (Fig.2).

Kinetic analysis of ActVB with a variety of flavin and NAD(P)H analogs allows the first detailed understanding of the protein-substrate interaction with this class of flavin reductases. Clearly the isoalloxazine ring provides a major site of interaction with the polypeptide chain. Lumiflavin, lacking a lateral chain, is a substrate and lumichrome and alloxazine are competitive inhibitors with respect to FMN, with K_d values comparable to the K_m value for lumiflavin (70-80 μM). In addition, the fact that K_d values for lumichrome and alloxazine are comparable shows that the methyl groups of the isoalloxazine ring at positions 7 and 8 are not important for the protein-flavin interaction. On the other hand, the K_m values for the natural substrates, riboflavin and FMN, are much lower (8 and 1 μM, Table III). Thus the ribityl chain also contributes to the binding. The catalytic efficiency of the enzyme with compound 1 and with FMN as substrates suggest that the 2'-OH of the sugar chain and the phosphate group play significant roles in the interaction of the substrate with the polypeptide chain. FMN is the better substrate in agreement with the finding that the purified preparations of ActVB contained FMN exclusively. This property represents a clear difference between the ActVB and the Fre flavin reductase families. Indeed, in the case of Fre, the recognition of the flavins occurs almost exclusively at the level of the isoalloxazine ring, with K_m values

for riboflavin and FMN comparable to that for lumiflavin and to the K_d value for the inhibitor lumichrome, in the 0.5-2 μM range (14).

The first and only available structural information on the ActVB family comes from the three dimensional structure of the Fer protein, from *Archaeoglobus fulgidus*, in complex with the FMN substrate (22). Since ActVB displays significant sequence homology with Fer (22% identity and 34% similarity, data not shown), it should be possible to identify some key residues for flavin binding in ActVB. However, this approach proved to be rather limited since the great majority of the residues involved in FMN binding in the Fer structure are not conserved in sequences of Fer homologs and many of these residues interact with FMN through main chain N and O atoms (22). Nevertheless, it is likely that ActVB should display structural similarities with Fer, with a FMN binding site that provides hydrogen bonds, ion pair interactions and electrostatic dipole interactions to the various parts of the substrate, the isoalloxazine ring, the OH groups of the ribitol chain and the phosphate group. In contrast, the structure of Fre, in complex with riboflavin, shows interactions of the polypeptide chain mainly with the isoalloxazine ring. All these results are consistent with the kinetic analysis reported here.

As far as the binding of reduced pyridine nucleotides is concerned, again large differences between the ActVB and the Fre families are observed. Whereas Fre recognizes NAD(P)H mainly through the nicotinamide ring, allowing NMNH to be a good substrate (17), ActVB interacts with the various parts of the

molecule. This is shown from the drastic increase of the K_d value for both inhibitors AMP and ADP-ribose and from the observation that NMNH is neither an inhibitor nor a substrate. It is also remarkable that ActVB is highly specific for NADH whereas Fre can use both NADH and NADPH. Again we learn very little from the structure of the homolog, the Fer protein from *A. fulgidus*, since the residues interacting with $NADP^+$, in a crystal of the Fer-FMN complex soaked with $NADP^+$, are not conserved in ActVB (22). However, as illustrated by the characterization of a strong charge-transfer complex between reduced flavin and NAD^+ in the active site of ActVB (Fig. 2 and 3), it is likely that, as in Fer, the nicotinamide ring of the pyridine nucleotide in ActVB packs against the isoalloxazine ring of the flavin, with the C4 atom of nicotinamide and the N5 atom of the flavin at a few Å from each other in a stacking arrangement typical for direct hydride transfer in flavoproteins. A specific structural analysis of ActVB is required to better understand the various aspects of substrate recognition and mechanism discussed above.

REFERENCES

1. Fontecave, M., Covès, J., and Pierre, J. L. (1994) *BioMetals* **7**, 3-8

2. Nivière, V., Vanoni, M. A., Zanetti, G., and Fontecave, M. (1998) *Biochemistry* **37**, 11879-11887

3. Ingelman, M., Ramaswamy, S., Nivière, V., Fontecave, M., and Eklund, H. (1999) *Biochemistry* **38**, 7040-7049

4. Covès, J., and Fontecave, M. (1993) *Eur. J. Biochem.* **211**, 635-641

5. Zenno, S., Saigo, K., Kanoh, H. and Inouye, S. (1994) *J. Bacteriol.* **176**, 3536-3543

6. Jeffers, C. E., and Tu, S.-C. (2001) *Biochemistry*,**40**, 1749-1754

7. Kendrew, S. G., Harding, S. E., Hopwood, D. A., and Marsh, E. N. G. (1995) *J. Biol. Chem.* **270**, 17339-17343

8. Thibaut, D., Ratet, N., Bish, D., Faucher, D., Debussche, L., and Blanche, F. (1995) *J. Bacteriol.* **177,** 5199-5205

9. Parry, R. J., and Li, W. (1997) *J. Biol. Chem.* **272**, 23303-23311

10. Galan, E. D., Prieto, M. A., and Garcia, J. L. (2000) *J. Bacteriol.* **182,** 627-636

11. Gray, K. A., Pogrebinsky, O. S., Mrachko, G. T., Xi, L., Monticello, D. J., and Squires, C. H. (1996) *Nature Biotechnol.* **14**, 1705-1709

12. Uetz, T., Schneider, R., Snozzi, M., and Egli, T. (1992) *J. Bacteriol.* **174,** 1179-1188

13. Witschel, M. Nagel, S., and Egli, T. (1997) *J. Bacteriol.* **179**, 6937-6943

14. Fieschi, F., Nivière, V., Frier, C., Décout, J. L., and Fontecave, M. (1995) *J. Biol. Chem.* **270**, 30392-30400

15. Eschenbrenner, M., Covès, J., and Fontecave, M. (1995) *J. Biol. Chem.* **270**, 20550-20555

16. Nivière, V., Fieschi, F., Décout, J. L., and Fontecave, M. (1996) *J. Biol. Chem.* **271**, 16656-1661

17. Nivière, V., Fieschi, F., Décout, J. L., and Fontecave, M. (1999) *J. Biol. Chem.* **274**, 18252-18260

18. Fontecave, M., Eliasson, R., and Reichard, P. (1987) *J. Biol. Chem.* **262**, 12325-12331

19. Zenno, S., and Saigo, K. (1994) *J. Bacteriol.* **176**, 3544-3551

20. Bruns, C. M., and Karplus, P. A. (1995) *J. Mol. Biol.* **247**, 125-145

21. Vadas, A., Monbouquette, H. G., Johnson, E., and Schröder, I. (1999) *J. Biol. Chem.* **274,** 36715-36721

22. Chiu, H. J., Johnson, E., Schröder, I., and Rees, D. C. (2001) *Structure.* **9,** 311-319

23. Laemmli, U. K. (1970) *Nature.* **227,** 680-685

24. Bradford, M. M. (1976) *Anal. Biochem.* **72**, 248-254

25. Segel, I. H. (1975) *Enzyme Kinetics*, John Wiley & Sons, New York

26. Massey, V., Matthews, R. G., Foust, G. P., Howell, L. G., Williams, C. H., Zanetti, G., and Ronchi, S. (1970) in *Pyridine Nucleotide-Dependent Dehydrogenases* (Sund, H., Ed.) pp 393-409, Springer-Verlag, Berlin

27. Zanetti, G., and Aliverti, A. (1991) In *Chemistry and Biochemistry of Flavoproteins, Vol. II* (Muller, F., Ed.) pp 306-312, CRC Press, Boca Raton

28. Rudolph, F. B., and Fromm, H. J. (1979) *Methods Enzymol.* **63**, 139-159

29. Dalziel, K. (1973) *The Enzymes,* 3nd Ed., Boyer, P. D., Ed., Vol. XI pp. 2-59, Academic Press, New York

30. Spector, T., and Cleland, W. W. (1981) *Biochem. Pharmacol.* **30**, 1-7

FOOTNOTES

This work has been supported by an Emergence Région Rhône-Alpes Fellowship.

FIGURE LEGENDS

Figure 1. Absorption spectra of the purified ActVB (60 μM in Tris/HCl 50 mM pH 7.6).

Figure 2. Anaerobic reduction of ActVB (130μM) containing FMN-bound (65μM) by NADH, in 50mM Tris/HCl buffer pH 7.6. Are shown, from top to the bottom at 455 nm, the spectra recorded after addition of a 0 (♦), 0.2, 0.4, 0.6, 0.8, 1, 1.1, and 1.3 (●) -fold molar excess of NADH with respect to FMN. In the inset is shown a plot of fractional absorbance changes observed at 455 nm, as a function of the [NADH]/[FMN] ratio.

Figure 3. Anaerobic titration of reduced ActVB-bound FMN with NAD^+. (○) Spectra of ActVB (130μM) containing oxidized FMN-bound (65μM) in 50mM Tris/HCl buffer pH 7.6, 5 mM EDTA and 1.4 μM 5-deazaflavin. (●) After irradiation for 30 min. After irradiation and anaerobic addition of 5 μM (△), 20 μM (□) and 70 μM (♦) NAD^+.

Figure 4. A, flavin reductase initial velocity v_i as a function of NADH concentration in the presence of 11 (○), 3.3 (Δ), 2.2 (●), 1.1 (□), 0.6 (♦) or 0.22 μM (◆) FMN. B, flavin reductase initial velocity v_i as a function of FMN concentration in the presence of 11 (○), 8.2 (Δ), 6.6 (●), 4 (□), 2 (♦) or 1.3

μM (◆) NADH. The flavin reductase concentration *e* used in these assays was 0.0545 μM. The results are presented in the form of double reciprocal plots.

Figure 5. A, AMP as a competitive inhibitor for NADH. The enzyme initial velocity v_i was assayed as a function of NADH concentrations using 7 μM FMN in the absence (○) or in the presence of 2 (Δ), 5 (●) or 7 mM (□) AMP. In the inset is shown a secondary plot of the slopes derived from Fig. 5A against [AMP], fitted with a straight line corresponding to the equation: $y = (K_m/V_m)(1+([I]/K_i))$. B, AMP as a noncompetitive inhibitor for FMN. The enzyme initial velocity v_i was assayed as a function of FMN concentrations using 40 μM NADH in the absence (○) or in the presence of 2 (Δ), 5 (●) or 7 mM (□) AMP. In the inset is shown a secondary plot of the intercepts derived from Fig. 5B against [AMP], fitted with a straight line corresponding to the equation: $y = (([I]/(K_i V_m)) + 1/V_m$. The flavin reductase concentration *e* used in these assays was 0.0545 μM. The results are presented in the form of double reciprocal plots.

Figure 6. A, lumichrome as a competitive inhibitor for FMN. The enzyme initial velocity v_i was assayed as a function of FMN concentrations using 40 μM NADH in the absence (○) or in the presence of 50 (Δ), 100 (●), 150 (□), 200 (♦) or 260 μM (◆) lumichrome. In the inset is shown a secondary plot of the slopes derived from Fig. 6A against [lumichrome], fitted with a straight line and corresponding to the equation: $y = (K_m/V_m)(1+([I]/K_i))$. B, lumichrome as an

uncompetitive inhibitor for NADH. The enzyme initial velocity v_i was assayed as a function of NADH concentrations using 7 μM FMN in the absence (○) or in the presence of 50 (Δ), 100 (●), 150 (□), 200 (♦) or 260 μM (◆) lumichrome. In the inset is shown a secondary plot of the intercepts derived from Fig. 6B against [lumichrome], fitted with a straight line corresponding to the equation: $y = (([I]/(K_i V_m)) + 1/V_m$. The flavin reductase concentration *e* used in these assays was 0.0545 μM.

Scheme 1. Structure of the different flavin (A) and pyridine nucleotide (B) analogs.

Table I

A. Purification of ActVB

Purification step	Protein (mg)	Activity [a] (μmol min^{-1})	Specific activity (μmol min^{-1} mg^{-1})	Recovery (%)
Soluble fraction	130	910	7	100
ACA 54	40	360	9	40
Superdex 75	3.6	61	17	6.7
UNO Q	1.8	57	32	6.2

B. Purification of ActVB-His

Purification step	Protein (mg)	Activity [a] (μmol min^{-1})	Specific activity (μmol min^{-1} mg^{-1})	Recovery (%)
Soluble fraction	180	900	5	100
Ni-NTA	11	308	28	34
UNO Q	8	280	35	31

[a] Enzyme activity was determined at 25 °C using the standard aerobic assay in the presence of 100 μM NADH and 50 μM FMN

Table II

Flavin reductase activity of different ActVB preparations, containing various amounts of bound FMN, measured in the presence of NADH (200 μM) and FMN (100 μM) or riboflavin (100 μM) as substrates, in 50 mM Tris/HCl pH 7.6.

Protein bound FMN (mol FMN/mol ActVB)	Specific activity (μmol min^{-1} mg^{-1})	
	FMN	Riboflavin
0.1	42	42
0.3	39	45
0.5	40	39
0.6	42	41

Table III

Apparent kinetic constants for various flavin derivates with NADH as electron donor [a]

Flavin derivate	Properties	K_m [b] (μM)	k_{cat} [b] (s^{-1})	K_i (μM)	K_d (μM)
Riboflavin	Substrate	8.1±0.9	13±0.6	-	-
FMN	Substrate	1.0±0.1	9.2±0.4	-	-
FAD	Substrate	8.7±0.6	8.2±0.7	-	-
Lumiflavin	Substrate	69±8	9.9±0.3	-	-
1	Substrate	3.7±0.4	8.1±0.2	-	-
2	Substrate	15.7±2.5	3.6±0.1	-	-
3	Substrate	11.4±0.8	7.2±1.3	-	-
Lumichrome [c]	Inhibitor competitive/FMN	-	-	104±17	87±14
Alloxazine [d]	Inhibitor competitive/FMN	-	-	93±19	78±18

[a] The enzyme preparation used in these experiments exhibited a slightly smaller specific activity than that used in the experiments reported in Table II.

[b] The concentration of NADH used for the determination of K_m and k_{cat} values was 200 μM.

[c] From the data of Fig. 6A.

[d] Experimental conditions as in Fig. 6A, except for alloxazine concentrations (0, 40, 90, 130 and 170 μM).

Table IV

Apparent kinetic and thermodynamic constants for NADH derivates with FMN as electron acceptor.

NADH derivate	Properties	K_m [a] (μM)	K_d (μM)
NADH	Substrate	6.6±0.5	7.8±0.7
AMP [b]	Inhibitor competitive/NADH	-	3000±500
ADP-ribose [c]	Inhibitor competitive/NADH	-	17400±4000
NADPH	Not a substrate up to 0.8 mM	-	-
NMNH	Not a substrate up to 1 mM Not an inhibitor up to 1 mM	-	-

[a] The concentration of FMN used for the determination of the K_m and k_{cat} values was 50 μM. k_{cat} value was 9.2 s^{-1}.

[b] From the data of Fig. 5A.

[c] Experimental conditions as in Fig. 5A, except for ADP-ribose concentrations (0, 0.8, 2 and 6 mM).

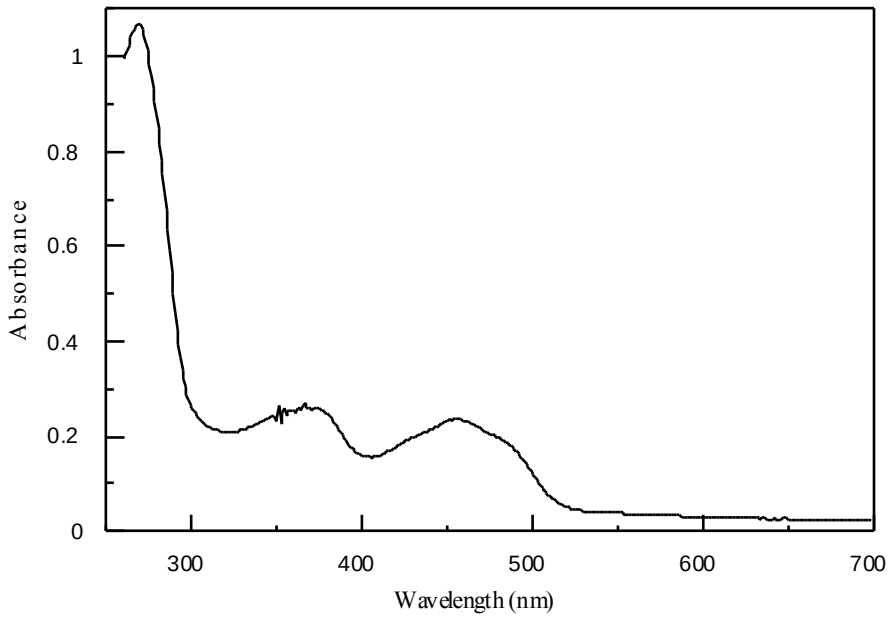

Figure 1

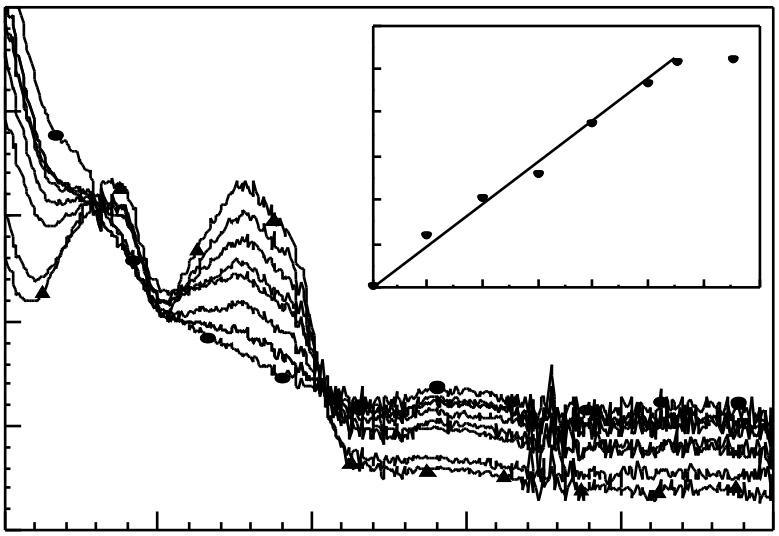

Figure 2

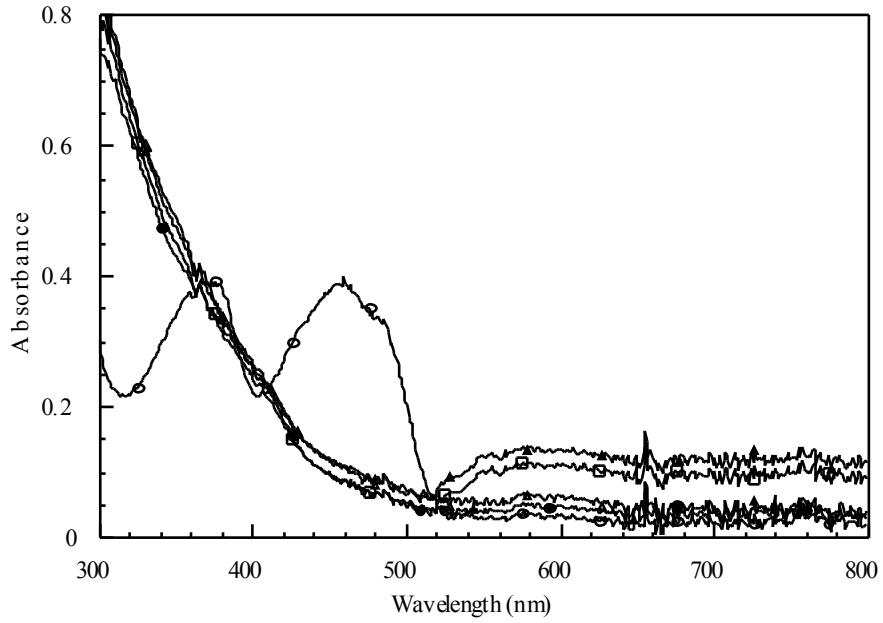

Figure 3

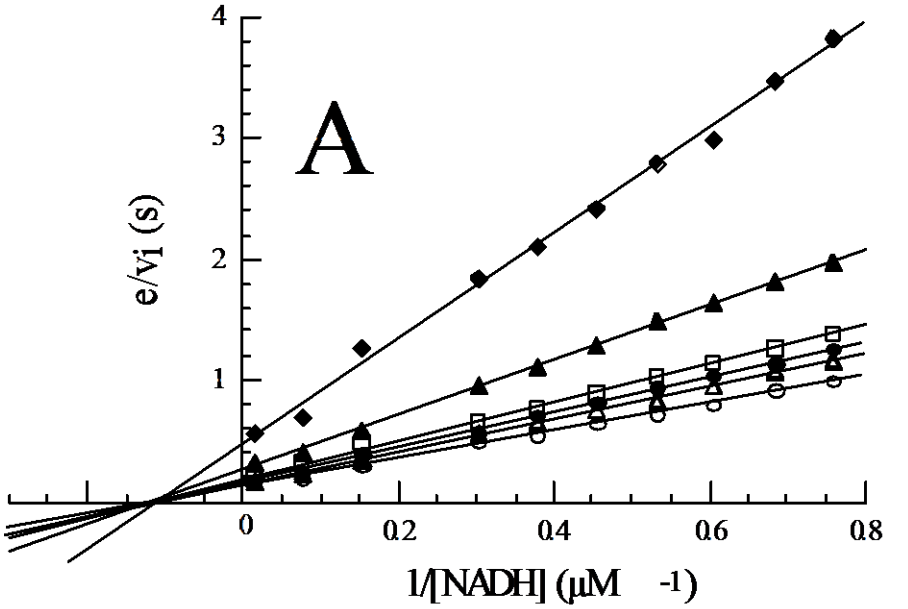

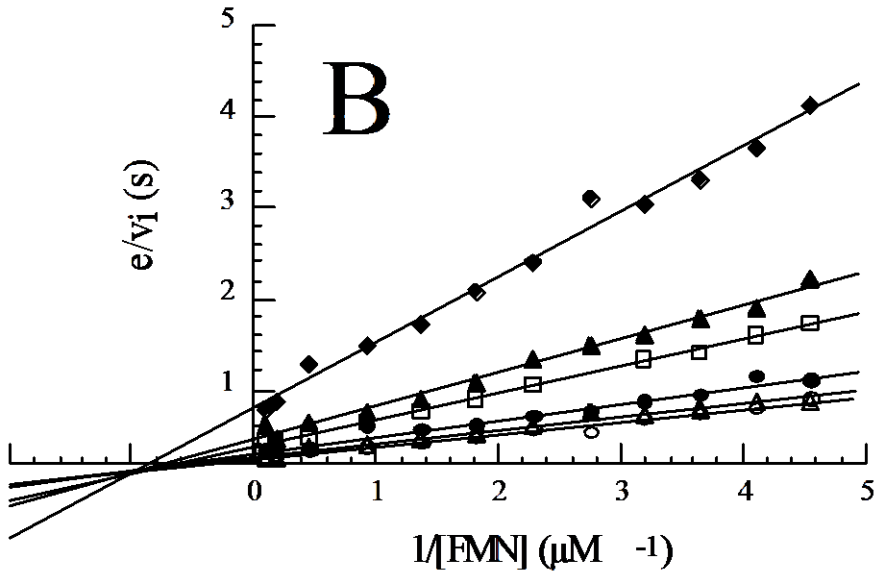

Figure 4

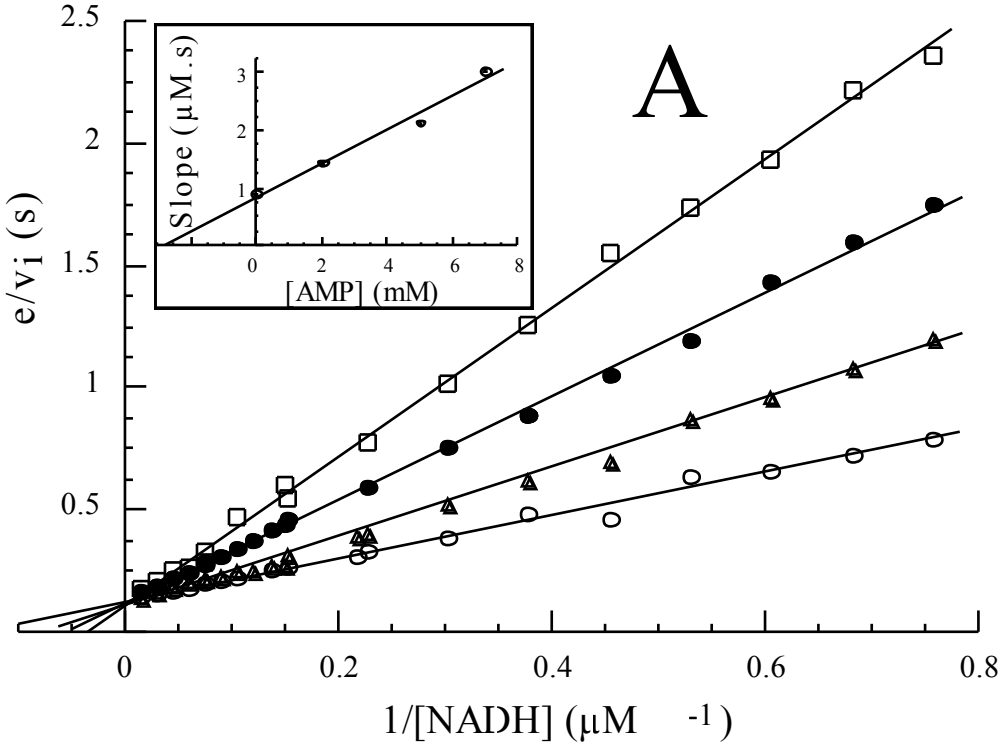
A
e/vi (s)
1/[NADH] (μM -1)
Slope (μM.s)
[AMP] (mM)

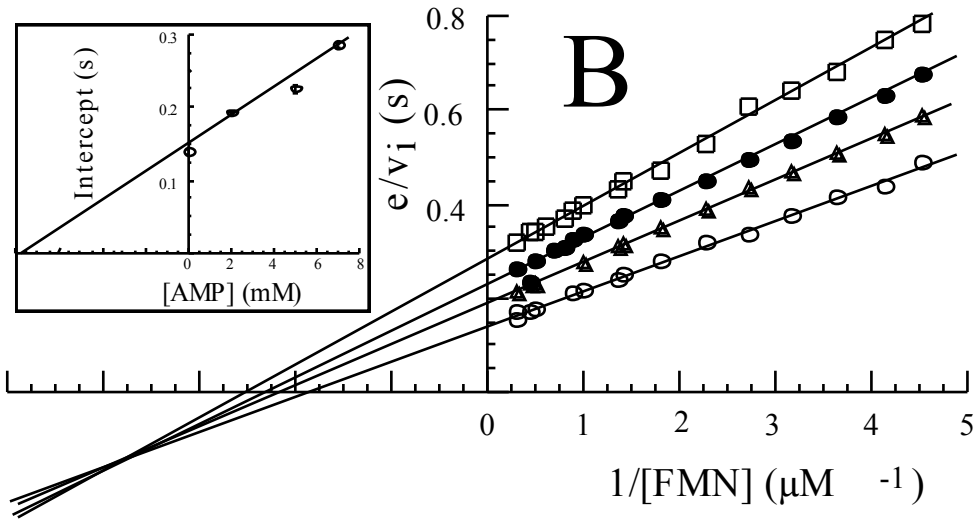
B
e/vi (s)
1/[FMN] (μM -1)
Intercept (s)
[AMP] (mM)

Figure 5

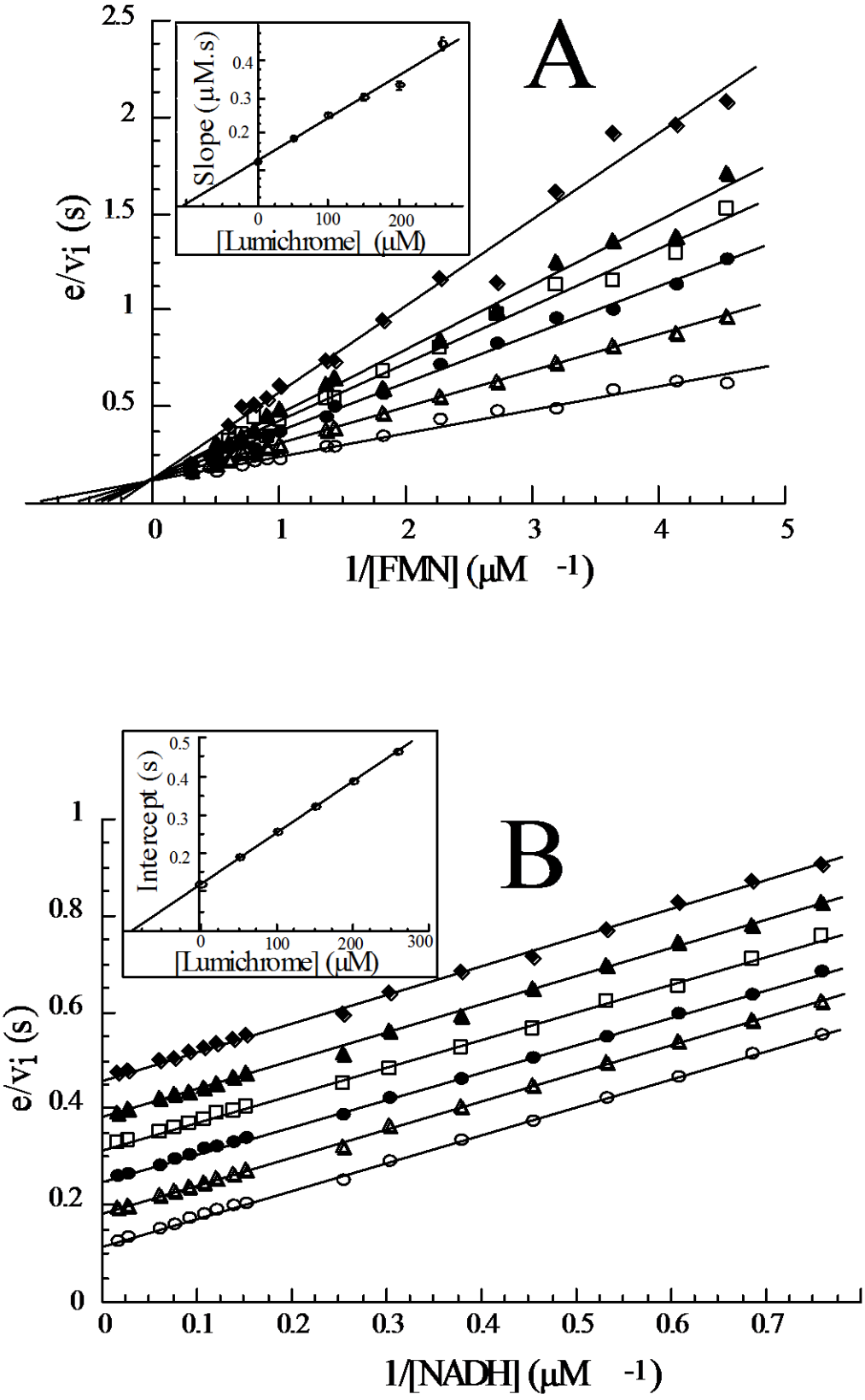
A
e/vi (s)
1/[FMN] (µM -1)
Slope (µM.s)
[Lumichrome] (µM)
B
e/vi (s)
1/[NADH] (µM -1)
Intercept (s)
[Lumichrome] (µM)

Figure 6

A

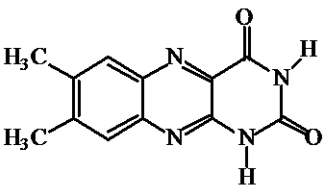

Lumichrome

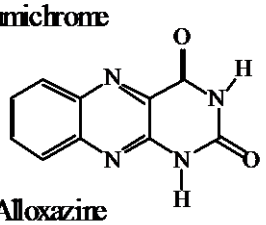

Alloxazine

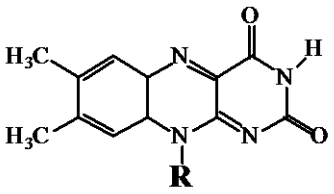

R=

CH_3 Lumiflavin

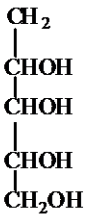

Riboflavin

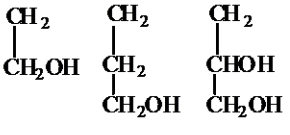

1 2 3

B

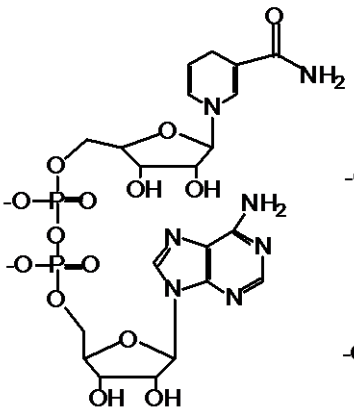

NADH

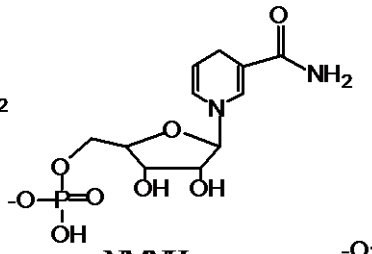

NMNH

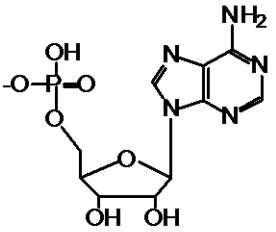

AMP

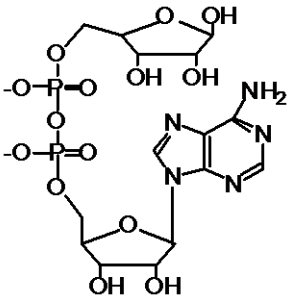

ADP-ribose

Scheme 1